

Geometric Control Theory and its Applications to Underwater Vehicles.

**A DISSERTATION PROPOSAL SUBMITTED TO THE GRADUATE COMMITTEE IN
PARTIAL FULFILLMENT OF THE REQUIREMENTS FOR THE DEGREE OF**

DOCTOR OF PHILOSOPHY

IN

OCEAN & RESOURCES ENGINEERING

by

Ryan N. Smith

Dissertation Committee:

Monique Chyba, Chair

(Department of Mathematics)

Song K. Choi

(Department of Mechanical Engineering)

R. Cengiz Ertekin

(Ocean & Resources Engineering Department)

Geno Pawlak

(Ocean & Resources Engineering Department)

George R. Wilkens

(Department of Mathematics)

Abstract

The proposed research is based on theoretical study and experiments which extend geometric control theory to practical applications within the field of marine science. In particular, we apply geometric methods to solve the motion planning problem for underwater vehicles. Bridging the gap between theory and application is the ultimate goal of control theory. Major developments have occurred recently in the field of geometric control which narrow this gap and which promote research linking theory and application. The work presented here is based on this recent progress with the objective to develop efficient tools for scientists and engineers in ocean research. On one hand, the underwater vehicle presents an ideal platform to extend known theory to mechanical systems which include dissipative and potential forces. And, on the other hand, the underwater vehicle application successfully demonstrates the applicability of geometric methods to design implementable motion planning solutions for concrete applications.

1 Goals, Objectives and Impact

RESEARCH GOAL 1.1. *It is a goal of this research to combine mathematics and ocean engineering through the application of differential geometry to the motion planning problem for underwater vehicles.*

RESEARCH OBJECTIVE 1.2. *It is an objective of this proposal to extend current results in geometric control theory to include potential and dissipative forces. In particular, we propose to provide an extension of controllability results for a submerged rigid body in an ideal fluid to motion planning solutions for a rigid body submerged in a viscous fluid including potential forces.*

We begin by considering the class of simple mechanical systems. A *simple* mechanical system is one which has a Lagrangian of the form kinetic minus potential energy. Simple mechanical systems are an important class of control systems including the rigid body, snakeboard, two-link manipulator, rolling disk and underwater vehicles. This class also contains the geometric structure of a Riemannian metric with the Levi-Civita affine connection *Do Carmo, 1992*. Using a differential geometry formulation of the simple mechanical system allows one to exploit nonlinear and geometric features inherent to the system which are not obvious in other mechanical control theory formulations.

For this theoretical analysis, a practical application is useful in order to visualize concepts and test results. The practical application we choose for this study is a submerged rigid body. This choice is motivated by the combined research interest in mathematics, engineering, mechanics and the ocean. Recent research has made great contributions to control theory using geometric framework with this application in mind *Bullo et al., 2002; Bullo and Lynch, 2001 and Bullo and Lewis, 2005*. However, the current results pertain to systems derived from a Lagrangian with no external or potential forces. In particular, the rigid body is submerged in an ideal fluid and added mass is usually neglected. Direct application of these results to a test-bed AUV is impossible due to obvious reasons. At least added mass, drag, buoyancy and gravitational forces must be considered in order to effectively and accurately implement controlled motions onto underwater vehicles. The extension of results for the rigid body submerged in an ideal fluid to the rigid body subjected to dissipative and potential forces from immersion in a viscous fluid is the main focus of this proposal.

Autonomous underwater vehicles (AUVs) are increasingly used, both in military and civilian applications. These vehicles are limited mainly by the intelligence we give them and the life of their batteries. Research is active to extend vehicle autonomy in both aspects. Our intent is to give the vehicle the ability to adapt its behavior under different mission scenarios (emergency maneuvers versus long duration monitoring). This involves a research and study of the motion planning problem for an underwater vehicle.

The motion planning problem for a submerged rigid body can be stated as follows: given an initial configuration (position and orientation) η_{init} at rest (i.e., the vehicle has zero velocity) and a final configuration η_{final} at rest, we are interested in finding motions to drive the body in the considered fluid from η_{init} to

η_{final} . After obtaining admissible motions from η_{init} to η_{final} , we can additionally include constraints and costs of which to optimize over a given trajectory. In this proposal, we are interested in finding motions which solve the motion planning problem and are derived using a geometric reduction procedure. It is also an interest of this research to establish a relationship between this geometric reduction and optimal control.

Traditionally, AUVs have taken the role of performing the long data gathering missions in the open ocean with little to no interaction with their surroundings, *MacIver et al., 2004*. The AUV is used to find the shipwreck, and a remotely operated vehicle (ROV) handles the up close exploration. AUV mission profiles of this sort are best suited through the use of a torpedo-shaped AUV since straight lines and minimal ($< 20^\circ$) angular displacements are all that are necessary to perform the transects and grid lines for these applications *Bertram and Alvarez, 2006*. However, a torpedo-shaped AUV lacks the ability to perform low-speed maneuvers in cluttered environments, such as autonomous exploration close to the seabed and around obstacles *MacIver et al., 2004*. Thus, a more versatile vehicle is necessary for more precise tasks. Also, motion planning for such a versatile vehicle is of great interest to the scientific community.

As their level of autonomy increases, AUVs will diversify the types of missions that they are able to perform. Some of these missions, as noted above, may be unsuitable for a traditional torpedo-shaped vehicle due to maneuverability constraints. Hence, we need to explore motions utilizing all six degrees of freedom in order to contribute to a more general class of underwater vehicles. Here we consider an agile vehicle capable of movement in six degrees of freedom without any preference of direction. We choose this versatility in order to consider the most general scenario in terms of actuation for the motion planning problem.

RESEARCH OBJECTIVE 1.3. *It is an objective to approach the motion planning problem for the submerged rigid body from a geometric control viewpoint and study trajectories for vehicles with unconstrained and unbiased movement in six degrees of freedom (DOF).*

During the past two decades, major developments have occurred in the field of geometric control and we propose to utilize these tools to develop new control strategies for a submerged rigid body. The use of such a framework gives a more in depth understanding of the geometric properties of the AUV as a mechanical system. We intend to exploit this geometric understanding to advance the theoretical intuition for the motion planning problem of the submerged rigid body.

Expanding our knowledge based on theory alone is insufficient, especially in such a practical field as AUV control. In parallel to theoretical study, we conduct weekly experiments on a test-bed AUV in order to validate our algorithms. These experiments are implemented onto the Omni-Directional Intelligent Navigator (ODIN), which is owned by the Autonomous Systems Laboratory, College of Engineering, University of Hawaii. Experiments are performed in the diving well at the Duke Kahanamoku Aquatic Complex.

RESEARCH IMPACT 1.4. *The impact of this proposed research would be felt in many areas of research. First, we expand the field of geometric control theory for the mathematics community. Also, we provide new control strategies for a submerged rigid body. These control strategies can then be exploited in many applications of AUVs in ocean research. Moreover, this research is not limited to ocean applications. As mentioned before, underwater vehicles are part of a larger group of mechanical systems subjected to external forces. The results of this research will be applicable to them as well. The strength of this proposal is not only in the impact upon different research areas, but also in that the results are both theoretical and applied in each research area.*

2 Statement of the Problem

The world's oceans cover over 75% of the earth's surface and are currently exploited for energy, recreation, transportation, food and much more. However, almost 95% of this vast resource is unexplored, *NOAA, 2004*.

Today’s maritime industries and research communities employ the use of underwater vehicles as a method to help discover the secrets of this abyss. Ocean research and exploration has evolved to the point that underwater vehicles are a necessity. In order to expand our knowledge base, we are pushing to go further and deeper than ever before. Among the many technological advances, AUVs are attracting recent research interests. The ability to reduce or eliminate the human factor in ocean research reduces exploration costs and risk to human life. For this proposal, we identify an AUV with its rigid body submerged in a viscous fluid. We focus our efforts on the ability of the AUV to design its own motion for a given scenario.

2.1 Hydromechanics of Underwater Vehicles

As stated in Research Objective 1.2, we wish to extend current controllability results for a submerged rigid body in an ideal fluid to obtain controllability results for a submerged rigid body in a viscous fluid. To this end, we will assume that the fluid is viscous and incompressible with the flow being rotational. Hereafter, we will refer to this medium as a *real* fluid. This characterization allows us to consider an AUV submerged in fresh or salt water as well as apply theoretical results to mechanical systems immersed in other fluids as well. Existing results in geometric control theory (e.g. *Bullo and Lewis, 2005*) are derived for the rigid body submerged in an ideal fluid and include terms such as added mass and inertia. However, potential forces and dissipative drag terms are neglected. Since it is an objective to apply the results of this research to a test-bed vehicle, we must include such external forces in order to make the theory practically applicable.

Our practical notion of a real fluid is water. In general, water is assumed to be inviscid, but for our application, there are viscous effects which can not be ignored. With regard to hydrostatics, the viscous fluid assumption does not affect the mass, displacement or righting moments. These quantities are unaltered from ideal fluid results. However, viscosity does affect the hydrodynamic forces and moments acting on a vessel. It is important to understand the effect of viscous and potential forces on the vehicle and how these translate to the equations of motion and the extension of existing geometric control theory results.

Since this research is a first extension of geometric control theory results to include potential and dissipative forces, we do not consider every possible force and moment induced. Here, we propose to extend current results by including added mass, which includes added mass moment of inertia, potential forces and moments including buoyancy and restoration forces and viscous drag forces. Understanding how to include these forces will open the possibilities to consider more complex forces and subtleties to create a more accurate theoretical model for the submerged rigid body.

2.2 Equations of Motion

The equations of motion for a submerged rigid body have been extensively studied, see e.g. *Fossen, 1994*. We will not repeat the derivation of these equations but rather highlight some of the geometrical features contained within these equations which will play a major role in our research.

We derive the equations of motion for a controlled rigid body immersed in an ideal fluid (air) and in a real fluid (water). Here, we consider water to be a viscous fluid (real fluid) in order to emphasize the inclusion of the dissipative terms in the equations of motion. This motivation comes from our desire to apply our results to the design of trajectories for test-bed underwater vehicles.

In the sequel, we identify the position and the orientation of a rigid body with an element of $SE(3)$: (b, R) . Here $b = (b_1, b_2, b_3)^t \in \mathbb{R}^3$ denotes the position vector of the body, and $R \in SO(3)$ is a rotation matrix describing the orientation of the body. The translational and angular velocities in the body-fixed frame are denoted by $\nu = (\nu_1, \nu_2, \nu_3)^t$ and $\Omega = (\Omega_1, \Omega_2, \Omega_3)^t$ respectively. Notice that our notation differs from the conventional notation used for marine vehicles. Usually the velocities in the body-fixed frame are denoted by (u, v, w) for translational motion and by (p, q, r) for rotational motion, and the spatial position

is usually taken as (x, y, z) . However, due to the geometric viewpoint taken, the chosen notation will prove more efficient, especially for the use of summation notation in our results.

It follows that the kinematic equations for a rigid body are given by:

$$\dot{b} = R\nu \quad (1)$$

$$\dot{R} = R\hat{\Omega} \quad (2)$$

where the operator $\hat{\cdot} : \mathbb{R}^3 \rightarrow \mathfrak{so}(3)$ is defined by $\hat{y}z = y \times z$; $\mathfrak{so}(3)$ being the space of skew-symmetric 3×3 matrices.

DEFINITION 2.1. *For this study, we refer to a configuration of the system as a six-tuple $\eta = (b, R)$ defining the position and orientation at a specific time. If the configuration is at rest we further assume that $\nu = \Omega = 0$.*

To derive the dynamic equations of motion for a rigid body, we let p be the total translational momentum and π be the total angular momentum, in the inertial frame. Let P and Π be the respective quantities in the body-fixed frame. It follows that $\dot{p} = \sum_{i=1}^k f_i$, $\dot{\pi} = \sum_{i=1}^k (\hat{x}_i f_i) + \sum_{i=1}^l \tau_i$ where f_i (τ_i) are the external forces (torques), given in the inertial frame, and x_i is the vector from the origin of the inertial frame to the line of action of the force f_i .

To represent the equations of motion in the body-fixed frame, we differentiate the relations $p = RP$, $\pi = R\Pi + \hat{b}p$ to obtain

$$\dot{P} = \hat{P}\Omega + E_F \quad (3)$$

$$\dot{\Pi} = \hat{\Pi}\Omega + \hat{P}\nu + \sum_{i=1}^k (R^t(x_i - b)) \times R^t f_i + E_T \quad (4)$$

where $E_F = R^t(\sum_{i=1}^k f_i)$ and $E_T = R^t(\sum_{i=1}^l \tau_i)$ represent the external forces and torques in the body-fixed frame respectively.

To obtain the equations of motion of a rigid body in terms of the linear and angular velocities, we need to compute the total kinetic energy of the system. The kinetic energy of the rigid body, T_{body} , is given by:

$$T_{body} = \frac{1}{2} \begin{pmatrix} v \\ \Omega \end{pmatrix}^t \begin{pmatrix} mI_3 & -m\hat{r}_{C_G} \\ m\hat{r}_{C_G} & J_b \end{pmatrix} \begin{pmatrix} v \\ \Omega \end{pmatrix} \quad (5)$$

where m is the mass of the rigid body, I_3 is the 3×3 -identity matrix and r_{C_G} is a vector which denotes the location of the body's center of gravity (C_G) with respect to the origin of the body-fixed frame. $J_b = \text{diag}(J_b^{\Omega_1}, J_b^{\Omega_2}, J_b^{\Omega_3})$ is the body inertia matrix. Based on Kirchhoff's equations (*Lamb, 1969*) we have that the kinetic energy of the fluid, T_{fluid} , is given by:

$$T_{fluid} = \frac{1}{2} \begin{pmatrix} v \\ \Omega \end{pmatrix}^t \begin{pmatrix} M_f & C_f^t \\ C_f & J_f \end{pmatrix} \begin{pmatrix} v \\ \Omega \end{pmatrix} \quad (6)$$

where $M_f = \text{diag}(M_f^{\nu_1}, M_f^{\nu_2}, M_f^{\nu_3})$, $J_f = \text{diag}(J_f^{\Omega_1}, J_f^{\Omega_2}, J_f^{\Omega_3})$ and C_f are respectively referred to as the added mass, the added mass moments of inertia and the added cross-terms.

The terms M_f, J_f, C_f all fall under the general description of added mass terms. The added mass is a pressure-induced force due to the inertia of the surrounding fluid and is proportional to the acceleration of the rigid body. In particular, the added mass μ_{ij} is the effective mass of the fluid that must be accelerated with the body. In the notation, the first subscript i refers to the *direction of the force/moment*, and the second subscript j refers to the *direction of motion*. The added mass coefficients are usually different

depending on the direction of translation. This is contrary to Newton's equation $F = ma$ where the mass, m , is independent of the direction of acceleration. Hence, this acts as the coefficient of proportion so that Newton's Laws hold in an ideal fluid. Without any symmetry, the cross-coefficients ($\mu_{12}, \mu_{13}, \mu_{23}$) are non-zero, which further asserts the fact that the hydrodynamic force differs in direction from the acceleration. However, the added mass coefficients do display symmetry ($\mu_{ij} = \mu_{ji}$) due to the absence of a free surface. This gives 21 independent coefficients; symmetry of the body further reduce the number of independent coefficients. In general, the added mass is given by:

$$\mu_{ij} = \rho \int_{S_B} \phi_j^{(R)} \frac{\partial \phi_i^{(R)}}{\partial n} dS, \quad (7)$$

where $\phi_i^{(R)}$ is the real part of the potential function describing the fluid surrounding the body. For this research, we assume a constant value for the added mass coefficients for ODIN, these are given by:

$$M_f^{\nu_i} = \mu_{ii} = \frac{1}{2} \rho \mathcal{V} = \frac{1}{2} \times 998 \times 0.14 \approx 70kg, \quad i = 1, 2, 3, \quad (8)$$

where \mathcal{V} is the submerged volume of the vessel.

The inertia term J_b is the resistance of a body to linear acceleration. We can represent the inertia tensor of a submerged body with reference to the body-fixed frame as:

$$\begin{bmatrix} I_x & -I_{xy} & -I_{xz} \\ -I_{yx} & I_y & -I_{yz} \\ -I_{zx} & -I_{zy} & I_z \end{bmatrix} \quad (9)$$

where I_x, I_y , and I_z are the inertia coefficients for the x, y , and z body-fixed directions respectively, and the remaining terms are the cross terms. We can calculate the above moments by:

$$I_x = \int_V (y^2 + z^2) \rho_A dV \quad (10)$$

$$I_y = \int_V (x^2 + z^2) \rho_A dV \quad (11)$$

$$I_z = \int_V (x^2 + y^2) \rho_A dV \quad (12)$$

where ρ_A is the mass density of the body. Note here that the mass of the body is given by:

$$m = \text{Mass}_{\text{ODIN}} = \int_V \rho_A dV \quad (13)$$

In our case, the inertia coefficients for ODIN are given by: $I_x = 5.46kg.m^2, I_y = 5.29kg.m^2, I_z = 5.72kg.m^2$ based on estimations of ODIN's mass density supplied by the Autonomous Systems Laboratory (ASL).

The added mass moment of inertia coefficients are the resistance of a body to angular acceleration. These coefficients, $J_f^{\Omega_i}, i = 1, 2, 3$, are commonly referred to as the added mass derivatives. As in *Imlay, 1961*, for a sphere, $J_f^{\Omega_i} = 0$ for $i = 1, 2, 3$. Thus, we take all of the added mass moment of inertia terms to be zero for ODIN. Note that for the added mass moment of inertia coefficients we do not consider the effects of appendages; ODIN is assumed to be a sphere.

Continuing on, we have obtained that the total kinetic energy of a rigid body submerged in an unbounded ideal or real fluid is given by:

$$T = \frac{1}{2} \begin{pmatrix} \nu \\ \Omega \end{pmatrix}^t \begin{pmatrix} \mathbb{I}_{11} & \mathbb{I}_{12} \\ \mathbb{I}_{12}^t & \mathbb{I}_{22} \end{pmatrix} \begin{pmatrix} \nu \\ \Omega \end{pmatrix}, \quad (14)$$

$$\begin{pmatrix} \mathbb{I}_{11} & \mathbb{I}_{12} \\ \mathbb{I}_{12}^t & \mathbb{I}_{22} \end{pmatrix} = \begin{pmatrix} mI_3 + M_f & -m\hat{r}_{C_G} + C_f^t \\ m\hat{r}_{C_G} + C_f & J_b + J_f \end{pmatrix} \quad (15)$$

This can also be written as $T = \frac{1}{2}(\nu^t \mathbb{I}_{11} \nu + 2\nu^t \mathbb{I}_{12} \Omega + \Omega^t \mathbb{I}_{22} \Omega)$. Using $P = \frac{\partial T}{\partial \nu}$ and $\Pi = \frac{\partial T}{\partial \Omega}$, we have:

$$\begin{pmatrix} P \\ \Pi \end{pmatrix} = \begin{pmatrix} mI_3 + M_f & -m\hat{r}_{C_G} + C_f^t \\ m\hat{r}_{C_G} + C_f & J_b + J_f \end{pmatrix} \begin{pmatrix} \nu \\ \Omega \end{pmatrix}. \quad (16)$$

The kinetic energy of a rigid body in an interconnected-mechanical system is represented by a positive-semidefinite $(0, 2)$ -tensor field on the configuration space Q . The sum over all the tensor fields of all bodies included in the system is referred to as the *kinetic energy metric* for the system. In this research, the mechanical system considered is composed of only one rigid body, the origin of the body fixed frame is located at C_G ($r_{C_G} = 0$) and the added cross terms C_f are zero. Then, the kinetic energy metric is the unique Riemannian metric on $Q = \mathbb{R}^3 \times \text{SO}(3)$ given by:

$$\mathbb{G} = \begin{pmatrix} M & 0 \\ 0 & J \end{pmatrix}, \quad (17)$$

where $M = mI_3 + M_f$ and $J = J_b + J_f$. In the sequel, we will use $m_i = m + M_f^{\nu_i}$ and $j_i = J_b^{\Omega_i} + J_f^{\Omega_i}$, for $i = 1, 2, 3$. Thus, $M = \text{diag}(m_1, m_2, m_3)$ and $J = \text{diag}(j_1, j_2, j_3)$. As with any Riemannian metric, associated to \mathbb{G} is its *Levi-Civita connection*: the unique affine connection that is both symmetric and metric compatible. The Levi-Civita connection provides the appropriate notion of acceleration for a curve in the configuration space by guaranteeing that the acceleration is in fact a tangent vector field along a curve γ ; the Levi-Civita connection can be studied in more depth in (*Bullo and Lewis, 2005*). The connection also accounts for the coriolis and centripetal forces acting on the system. Explicitly, if $\gamma(t) = (b(t), R(t))$ is a curve in $\text{SE}(3)$, and $\gamma'(t) = (\nu(t), \Omega(t))$ is its pseudo-velocity as given in Equations 1 and 2, the acceleration is given by

$$\nabla_{\gamma'} \gamma' = \begin{pmatrix} \dot{\nu} + M^{-1}(\Omega \times M\nu) \\ \dot{\Omega} + J^{-1}(\Omega \times J\Omega + \nu \times M\nu) \end{pmatrix}, \quad (18)$$

where ∇ denotes the Levi-Civita connection and $\nabla_{\gamma'} \gamma'$ is the covariant derivative of γ' with respect to itself.

In order to consider rigid body motion in a viscous fluid, we must incorporate external interaction into the above equations of motion. These interactions come in the form of control inputs, buoyancy and friction, among others. These are characterized as forces. Since this theory is based in the calculus of variations, the notion of a force is not as obvious as when viewed from the Newtonian point of view. The following describes how we incorporate external forces into the Lagrangian framework and geometric equations of motion.

Suppose that a rigid body is subjected to a Newtonian force (N_f) or torque (N_t). We allow a general external force F to depend on position ($(b, R) \in \mathbb{R}^3 \times \text{SO}(3)$), on velocities ($(\dot{b}, \dot{R}) \in T_{(b,R)}(\mathbb{R}^3 \times \text{SO}(3))$) and on time. So, for each $v_q \in TQ$, we define an element $F_{N_f, N_t}(t, v_q) \in T_q^*Q$ which models the effects of N_f and N_t in the differential geometry framework.

DEFINITION 2.2. (*Force*)(*Bullo and Lewis, 2005, p. 189*) For $r \in \mathbb{N} \cup \{\infty\}$, a C^r -force on a manifold Q is a map $F : \mathbb{R} \times TQ \mapsto T^*Q$ with the property that F is a locally integrally class C^r bundle map over id_Q . A C^r -force is

- time-independent if there exists a C^r -fiber bundle map $F_0 : TQ \mapsto T^*Q$ over id_Q with the property that $F(t, v_q) = F_0(v_q)$, and is
- basic if there exists a C^r -covector field F_0 on Q such that $F(t, v_q) = F_0(q)$.

If $\gamma : I \mapsto Q$ is a C^r -curve, then a C^r -force along γ is a C^r -covector field $F : I \mapsto T^*Q$ along γ .

Now, let X_1, \dots, X_6 be the standard left-invariant basis for $SE(3)$ and let π^1, \dots, π^6 be it's dual basis. Then, we can express an external force acting on the system as a one form

$$F_{N_f, N_t}(t, v_q) = \sum_{i=1}^6 F_i(t, b, R, \nu, \Omega) \pi^i, \quad (19)$$

where F_i is the i^{th} component of the force, $i = 1, \dots, 6$. This force lives on T^*M . In order to express a force as an acceleration, we must divide by the mass, remember Newton's $F = ma$. This is accomplished by applying $\mathbb{G}^\#$, the inverse of the kinetic energy metric \mathbb{G} . Multiplication by the matrix $\mathbb{G}^\#$ represents a vector bundle isomorphism from T^*M to TM which essentially means divide by mass.

$$\mathbb{G}^\# = \text{diag} \left(\frac{1}{m_1}, \frac{1}{m_2}, \frac{1}{m_3}, \frac{1}{j_1}, \frac{1}{j_2}, \frac{1}{j_3} \right). \quad (20)$$

In matrix form, we write the the external forces as geometric acceleration as

$$\mathbb{G}^\#(F(\gamma'(t))) = \text{diag} \left(\frac{F_1}{m_1}, \frac{F_2}{m_2}, \frac{F_3}{m_3}, \frac{F_4}{j_1}, \frac{F_5}{j_2}, \frac{F_6}{j_3} \right). \quad (21)$$

We now consider the forces and torques specific to the research in this proposal.

We first consider those forces which arise from a potential function. These potential forces can be viewed as a force (torque) which acts to pull the rigid body back to an equilibrium position or orientation. Potential functions are commonly known to store energy to be turned into kinetic energy later. In particular, given a potential function $V \in C^\infty(Q)$ on Q its *potential force* is the basic force (see Def. 2.2) given by $F(t, v_q) = -dV(q)$. In this study, we concern ourselves with potential forces which are independent of time and velocity. The theory supports potential functions which do depend on position, velocity and time, however, our application does not require considering these cases.

In the case of the submerged rigid body we encounter a potential force and a potential torque. The potential force arises from the acceleration due to gravity and the buoyancy force exerted by the fluid upon the submerged volume of the vessel. This force acts directly on C_G , and is given by the potential function $V_B(\gamma(t)) = W - \rho g \mathcal{V}$ where W is the weight of the rigid body, ρ is the fluid density, g is the acceleration due to gravity and \mathcal{V} is the submerged volume of the body.

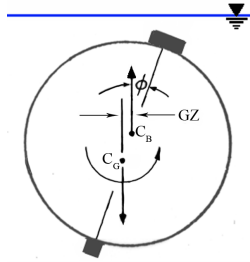


Figure 1: Righting arm (GZ) for a submerged spherical vehicle.

The potential torque also arises from the gravity and buoyancy forces, but in the form of the righting moment. The moment arm is created by a separation of C_G and the center of buoyancy C_B . This acts to

right the vessel upon listing; see Figure 1. The righting action is a pure torque applied to C_G acting to restore angular displacements. This torque is given, in two dimensions, by the potential function $Y(\gamma(t)) = W * GZ = \rho g(C_G - C_B) \sin(\phi)$, where GZ is the distance between the vertical line through C_G pointing in the direction of gravity and the vertical line through C_B pointing in the direction of gravity and ϕ is the list angle of the vessel. In the equations of motion we will separate the two potential forces defined above since their actions depend on different assumptions on the rigid body.

The potential force of buoyancy/gravity is expressed as an acceleration in our equations of motion by the gradient vector field of the potential function $V_B(\gamma(t)) = W - \rho g \mathcal{V}$. We denote the potential acceleration as $-\mathbb{G}^\# dV_B = -\text{grad } V_B(\gamma(t))$ for $V_B \in \mathcal{C}^\infty$. The potential torque (righting moment), written as a geometrical acceleration is given by $Y(\gamma(t)) = (0, 0, 0, -r_{C_B} \times R^t \rho g \mathcal{V} k)^t$ where k the unit vector pointing in the direction of gravity.

We note here that not all external forces interacting with a submerged rigid body can be derived from a potential function. One example is the external force due to friction, or in our specific case, viscous drag. This force arises due to the friction caused by the viscosity of the surrounding fluid. Such a force is called a dissipative force since it dissipates energy from the system.

It is commonly known in hydrodynamics that drag forces are proportional to the square of the velocity of the body. In this paper, we make the assumption that we have a drag force $D_\nu(\nu)$ and a drag momentum $D_\Omega(\Omega)$ implying that there are no off-diagonal terms. The contribution of these forces is quadratic with respect to the respective velocities, for example

$$D_\nu(\nu_1) = C_D \rho A \nu_1^2, \quad (22)$$

where C_D is the drag coefficient for the sphere and its appendages as estimated using *Allmendinger, 1990*, ρ is the density of the fluid, A is the projected surface area of the body in the direction of the velocity, ν_i are the translational velocities and Ω_i are the rotational velocities. Here, we assume that form drag is dominant for our application (specific AUV test-bed) and our estimations of this include any other drag terms (such as fluid shear stresses due to rotational viscous flow).

REMARK 2.3. *Note that in Equation 22, we express the drag force as quadratic with respect to velocity using ν^2 as opposed to $\nu|\nu|$. This assumption is valid since the trajectories we will consider are concatenations of decoupling vector fields. Along each component of the trajectory, we will only allow movement in one direction for a given velocity component. Thus, we are always sure that the drag force will be a dissipative force for that motion.*

Generally, a vehicle will have different drag coefficients and different projected areas depending on the direction of the velocity, we define $D_i = C_{D_i} \rho A_i$ where $i \in \{1, \dots, 6\}$ denotes the direction of the velocity. Then we let $\mathcal{D}_i = -\frac{D_i}{m_i} \nu_i^2$ for $i = 1, 2, 3$ and $\mathcal{D}_i = -\frac{D_i}{j_{i-3}} \Omega_{i-3}^2$ for $i = 4, 5, 6$. Now, we can write $F_{drag}(\gamma'(t)) = \sum_{i=1}^6 F_i(\gamma'(t)) \pi^i(\gamma'(t))$ which expands to $F_{drag}(\gamma'(t)) = \sum_1^3 F_i(\gamma'(t)) \nu_i^2 \pi_i + \sum_{i=1}^3 F_{i+3}(\gamma'(t)) \Omega_i^2 \pi_i$.

Thus, we compute $\mathbb{G}^\#(F_{drag}(\gamma'(t))) = \sum_{i=1}^3 \frac{F_i(\gamma'(t))}{\mathbb{G}_{ii}} \nu_i^2 X_i + \sum_{i=4}^6 \frac{F_i(\gamma'(t))}{\mathbb{G}_{ii}} \Omega_{i-3}^2 X_i = \sum_{i=1}^6 \mathcal{D}_i X_i$ where \mathbb{G}_{ij} is the i, j -entry of the kinetic energy matrix \mathbb{G} as given before. The result is the drag force expressed as a geometric acceleration given by $\mathbb{G}^\#(F_{drag}(\gamma'(t))) = \sum_{i=1}^6 \mathcal{D}_i X_i$ which we can now incorporate into the differential geometric equations of motion.

The final external forces which we consider are the control forces. These are the forces to which we supply the inputs to move the rigid body through the surrounding fluid. Throughout this paper, we assume that we have three forces acting at the center of gravity along the body-fixed axes and that we have three pure torques about these axes. We will refer to these controls as the six degree of freedom (DOF) controls. We denote the controls by: $\sigma = (\varphi_\nu, \tau_\Omega) = (\varphi_{\nu_1}, \varphi_{\nu_2}, \varphi_{\nu_3}, \tau_{\Omega_1}, \tau_{\Omega_2}, \tau_{\Omega_3})$.

REMARK 2.4. *The above notion of control forces is not realistic from a practical point of view since underwater vehicle controls may represent the action of the vehicle's thrusters or actuators. The forces from these actuators generally do not act at the center of gravity and the torques are obtained from the momenta created by the forces. As a consequence, to set up experiments with a real vehicle, we must compute the transformation between the six DOF controls and the controls corresponding to the thrusters. We address such a transformation for our actual test-bed vehicle in Equations (29) and (30) as well as in Chyba et al., 2007a and Chyba et al., 2007b.*

DEFINITION 2.5. *The equations of motion for a general simple mechanical control system (rigid body) submerged in a real fluid subjected to external forces can be written as*

$$\nabla_{\gamma'} \gamma' = (-\text{grad } V_B(\gamma(t))) + \mathbb{G}^\#(F(\gamma'(t))) + Y(\gamma(t)) + \sum_{i=1}^6 \mathbb{I}_i^{-1}(\gamma(t)) \sigma_i(t), \quad (23)$$

where $\text{grad } V_B(\gamma(t))$ represents the potential force arising from gravity and the vehicle's buoyancy, $\mathbb{G}^\#(F(\gamma'(t)))$ represents the dissipative drag force, $Y(\gamma(t)) = (0, 0, 0, -r_{C_B} \times R^t \rho g \mathcal{V} k)^t$ accounts for any induced righting moment, $\mathbb{I}_i^{-1} = \mathbb{G}^\# \pi_i = \mathbb{G}^{ij} X_j$, which may be represented as the i^{th} column of the matrix $\mathbb{I}^{-1} = \begin{pmatrix} M^{-1} & 0 \\ 0 & J^{-1} \end{pmatrix}$, and $\sigma_i(t)$ accounts for the control.

Note that for a neutrally buoyant vessel, Equations (23) are equivalent to

$$M\dot{\nu} = M\nu \times \Omega + D_\nu(\nu)\nu + R^t \rho g \mathcal{V} k + \varphi_\nu \quad \text{and} \quad (24)$$

$$J\dot{\Omega} = J\Omega \times \Omega + M\nu \times \nu + D_\Omega(\Omega)\Omega - r_B \times R^t \rho g \mathcal{V} k + \tau_\Omega, \quad (25)$$

which are the form of the equations of motion usually encountered in the literature. We refer interested readers to *Catone et al., 2007 and Chyba et al., 2007c and Leonard, 1996 and Leonard, 1997* for an in depth treatment of the geometric features of submerged rigid bodies.

2.3 Real Fluid

The above discussion details the general equations of motion for rigid body motion in a viscous fluid. In the sequel, we may make some assumptions which simplify these equations slightly. If assume that the rigid body is neutrally buoyant, we eliminate the external potential force $V_B(\gamma(t)) = W - \rho g \mathcal{V}$. If we also assume that $C_G = C_B$, this eliminates the restoring moment $Y(\gamma(t))$. Under both of these assumptions, we rewrite Equation (23) as

$$\nabla_{\gamma'} \gamma' = \mathbb{G}^\#(F(\gamma'(t))) + \sum_{i=1}^6 \mathbb{I}_i^{-1}(\gamma(t)) \sigma_i(t), \quad (26)$$

2.4 Ideal Fluid

For rigid body motion in an ideal fluid, the lack of viscosity allows us to neglect the external dissipative drag force. In the absence of this drag force, we can write the equations of motion as follows:

$$\nabla_{\gamma'} \gamma' = -(\text{grad } V_B(\gamma(t))) + Y(\gamma(t)) + \sum_{i=1}^6 \mathbb{I}_i^{-1}(\gamma(t)) \sigma_i(t). \quad (27)$$

Under both assumptions listed at the beginning of Section 2.3, we can rewrite Equation (27) without the potential force and restoring moment as

$$\nabla_{\gamma'} \gamma' = \sum_{i=1}^6 \mathbb{I}_i^{-1}(\gamma(t)) \sigma_i(t). \quad (28)$$

PROPOSED PROBLEM 2.6. Given η_{init} and η_{final} both at rest, we seek controls σ_i which steer the system governed by Equations (23) from η_{init} to η_{final} .

To solve this problem, we consider first the system governed by Equations (28). We can then add external forces until we reach the full extent of the system governed by Equations (23).

3 Previous Work

The proposed Problem 2.6 has been previously addressed as an optimal control problem in *Chyba et al., 2007a* and *Chyba et al., 2007b*. These papers focus mainly on time minimization and the development of a numerical algorithm which produces implementable trajectories. The minimization of energy consumption along trajectories of the system is also explored. Many trajectories based on these papers have been successfully implemented onto ODIN with excellent results (see Figure 2). Figure 2 displays the experimental (solid

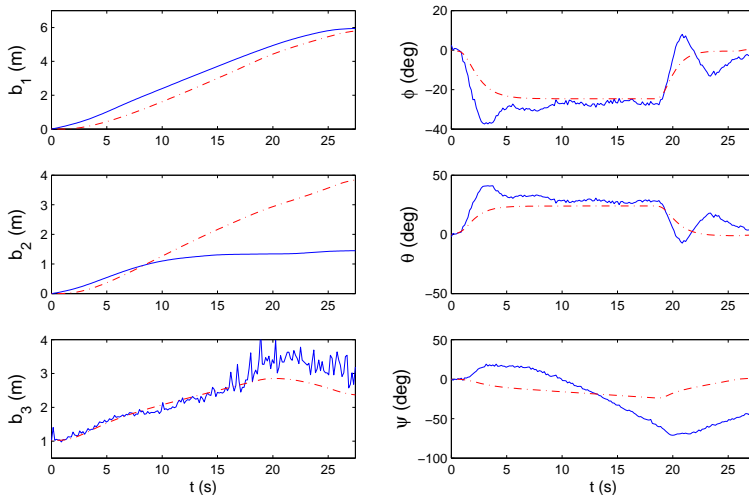


Figure 2: *Experimental (solid) and theoretical (dashed) evolutions of the AUV for the $(STPP)_2$ strategy targeting $\eta_T = (6, 4, 1, 0, 0, 0)$.*

line) and theoretical or prescribed (dashed line) evolution of the vehicle. Here the vehicle configuration is given by $\eta(t) = (b_1(t), b_2(t), b_3(t), \phi(t), \theta(t), \psi(t))$ where ϕ , θ and ψ are the usual Euler angles. We modify the theoretical evolution by an initial rotation to match the orientation ODIN started with in the pool. Before analyzing the experimental data, we emphasize that ODIN operates in a completely open loop framework with no feedback controls. All controls are computed before the experiment. We first note that the evolution of the yaw does not have the same general trend as the prescribed strategy. This is nearly impossible to fix since there are minimal restoring forces acting in this direction. Any misappropriated horizontal thrust results in a parasite yaw torque. This significantly affects the yaw evolution since there are no counteracting forces or moments. Note that all other components do not exactly match the prescribed motion, but follow the general trend of the trajectory. Parasite torques exist for roll and pitch but are far less problematic due to the restoring moment created by $|C_G - C_B| \neq 0$. The restoring moments make pitch and roll parasite torques negligible. As for the evolution of ϕ (roll) and θ (pitch), we see that the experimental data agrees with the theoretical prediction except in the two instances of overshoot at $\approx 2sec$ and $\approx 20sec$. These over-shootings arise for three main reasons. The first reason is simply the overshooting of the thrusters.

This indicates that the 0.9 s linear junction inserted between thrust arcs to eliminate instantaneous switching of the thrusters does not completely erase the transient response of the thrusters. However, using a larger duration for this junction would render the time efficient control strategy less time efficient and may even impair its convergence. The second identified reason is the sensor accuracy and transient behavior. We have conducted many experiments and concluded that in the yaw direction, the inertial measurement sensor is prone to misreading during rapid changes of orientation. This effect occurs in pitch and roll, but is less obvious due to the righting moment. A final reason would be an over estimation of the drag coefficient in pitch and roll (and then in yaw by symmetry). Indeed the observed overshooting looks very similar to what would happen to a less damped system. Future experiments will determine the respective impact of these three issues as this is a work in progress.

The depth evolution (b_3) looks fine until about 20 s when ODIN dove more than expected. This is caused by the instability of the thrusters around a switching coupled with overshooting based again on drag estimates. We are also examining the effect of the tether on the buoyancy of ODIN. For the horizontal motions, we note a good comparison in surge, while the sway evolution leaves much to be desired. However, with the overshooting issue in pitch and roll, we can not expect to match both surge and sway evolutions simultaneously at this point.

Despite the mentioned differences between the theoretical and experimental evolution of ODIN, the results are still quite impressive. What we point out above are issues which can be resolved through continued testing and vehicle updates which are discussed in Section 4.4. Through the previous testing and experimentation, we have worked out many of the bugs and glitches over the past few months. This makes ODIN an excellent platform with which to begin applying more theoretically derived motions since her behavior is very well known and documented.

One aspect of the physical system that we have spent considerable time on is the physical thruster modeling. This begins with the fact that from Section 2.2 we assume that the vehicle is controlled by three translational forces and three rotational moments applied directly at C_G . In application we know that this is rarely the case. For ODIN, we have eight external thrusters not located at C_G which apply the forces and torques for movement. To remedy this we have a transformation from the the eight dimensional thruster actuation to the six dimensional theoretical controls using the following Thrust Control Matrices (TCM's) (Eqns. 29 and 30). These matrices were computed by translating a force from a thruster at its given position on ODIN to its corresponding force and torque at center of gravity.

$$TCM \text{ horizontal} = \begin{bmatrix} -0.707 & 0.707 & 0.707 & -0.707 \\ 0.707 & 0.707 & -0.707 & -0.707 \\ 0.48160 & -0.48160 & 0.48160 & -0.48160 \end{bmatrix} \quad (29)$$

$$TCM \text{ vertical} = \begin{bmatrix} -1.0 & -1.0 & -1.0 & -1.0 \\ -0.26989 & -0.26989 & 0.26989 & 0.26989 \\ 0.26989 & -0.26989 & -0.26989 & 0.26989 \end{bmatrix} \quad (30)$$

An additional constraint regarding the physical thrusters on ODIN is that the thrusters have output limitations and the input voltage to output force functions are unique and highly nonlinear. The thrusters can not switch direction instantaneously nor is the output thrust symmetric about zero. It is impossible to implement a continuous evolving strategy (singular arc) due to on board data storage limitations and computational resources.

We have been able to position C_G with respect to C_B in order to fine tune the desired balance between the controllability and stability of ODIN. Since we consider such a versatile vehicle for application, we had some issues with positioning in the $x - y$ plane (horizontal position). Global positioning systems are greatly affected by the pool circulation pumps and do not give good accuracy without expensive differential correction hardware. Also, the penetration of the signal into water is not reliable. Sonar sensors created too much noise in the diving well to give precise readings, and were rendered useless if ODIN pitched or

rolled more than about 5° . Many other methods were investigated including cameras, lasers and USBL systems. We were unable to find an affordable, accurate and easily implementable solution to give real time feedback. Thus, we have solved the problem by video taping the experiments from the 10m diving platform. This gives a near nadir view of the experimentation area, and we are able to determine ODIN's relative position in the pool accurately to within 10cm. This is a post processed method, so we are unable to supply horizontal feedback to our vehicle during experiments. This situation forced us to create an accurate hydrodynamic model of ODIN since all trajectories are performed in open loop. This hydrodynamic model was first estimated following procedures outlined in (*Allmendinger 1990, Bhattacharyya 1978, Imlay 1961, Lamb 1945*) and were updated through model testing on a one to one scale. For the numerically computed time minimal trajectories, we found that we could model the drag using a cubic function with no quadratic or constant term. This relationship is beneficial since representing drag by $= \frac{1}{2}C_D\rho AU|U|$ (with U representing velocity) gives a non-differentiable function which is impossible to deal with in numerical computations.

Even though these experimental data have matched the theoretical predictions very well, the trajectory design is based on numerical computations which leaves us without a complete understanding of the system from a theoretical point of view. It is this complete understanding which we seek in order to be able to fully apply the techniques of geometric control. Through months of weekly testing and observation, the vehicle limitations are well known and accounted for. Now, through the proposed research, we wish to give a better understanding of the underwater vehicle submerged in a real fluid from a theoretical point of view in order to advance the implementation of efficient trajectories. Also, current study has revealed that investigation into the under-actuated scenario may be of interest. Not only would researching the under-actuated situation aide motion planning in a time of actuator failure or vehicle distress, but it may also help merge the geometric theory with the practical application for the fully-actuated scenario as well.

4 Proposed Research

In order to accomplish the proposed goals and objectives from Section 1 we will attack Problem 2.6 by examining geometric reduction procedures for the control system derived in Section 2.2 for the rigid body submerged in a real fluid. A first step toward the development of the geometric reduction procedures for systems including dissipative and potential forces is to first consider the ideal fluid case where these drag forces are not present (ie. the system is governed by Equations (27)). A further simplification is to assume that C_G and C_B coincide, and that the body is neutrally buoyant (ie. the system is governed by Equations (28)). Under the later assumptions, we have an affine connection control system, and existing theory can be applied. We then propose to include external potential and dissipative forces one at a time to extend existing theory step by step. Understanding the simple case first will aide the development of extensions to more general situations, such as the systems governed by Equations (23). Research has been active by the candidate to accomplish this initial stage of research *Catone et al., 2007*, and the results are summarized in the following sections. We note once again that from this point, until specified otherwise, we consider a neutrally-buoyant rigid body submerged in an ideal fluid with $C_G = C_B$. We will later generalize these assumptions.

4.1 Decoupling Vector Fields

In order to discuss the initial results referred to above, it is necessary to introduce some notation and terminology. Here we keep the application in mind, but will present the concepts in general terms. From Section

2.2 it is clear that a general affine-connection control system can be expressed as:

$$\nabla_{\gamma'(t)}\gamma'(t) = \sum_{a=1}^k u^a(t)Z_a(\gamma(t)), \quad (31)$$

where $u^1(t), \dots, u^k(t)$ are measurable controls and Z_1, \dots, Z_k are independent vector-fields defined on the configuration space Q that span $\mathcal{Z} \subset TQ$, a constant-rank distribution. In *Bullo and Lewis, 2005* the authors introduce the notion of kinematic reductions which are the foundation for the geometric reductions mentioned earlier. Decoupling vector fields are kinematic reductions of rank one. We make this more precise with the following definition.

DEFINITION 4.1. *A decoupling vector field for an affine-connection control system is a vector field V on Q having the property that every reparameterized integral curve for V is a trajectory for the affine-connection control system. More precisely, let $\gamma : [0, S] \rightarrow Q$ be a solution for $\gamma'(s) = V(\gamma(s))$ and let $s : [0, T] \rightarrow [0, S]$ satisfy $s(0) = s'(0) = 0$, $s(T) = S$, $s'(t) > 0$ for $t \in (0, T)$, and $(\gamma \circ s)' : [0, T] \rightarrow TQ$ is absolutely continuous. Then $\gamma \circ s : [0, T] \rightarrow Q$ is a trajectory for the affine-connection control system.*

A necessary and sufficient condition for V to be a decoupling vector field for the affine-connection control system (31) is that both V and $\nabla_V V$ are contained in \mathcal{Z} (*Bullo and Lewis 2005*). Notice that if $\mathcal{Z} = TQ$ then the system is fully-actuated and every vector field of \mathcal{Z} is a decoupling vector field, and if $\mathcal{Z} = \text{span}\{Z\}$ then V is a decoupling vector field if and only if both V and $\nabla_V V$ are multiples of Z . Decoupling vector fields are found by solving a system of homogeneous quadratic polynomials in several variables and are of most interest when considering an under-actuated scenario.

In the case of the submerged rigid body, Equation (31) can be represented as a *fully-actuated* affine-connection control system given by Equation (28). In this case, there are no quadratic polynomials to solve and every left-invariant vector field is a decoupling vector field. However, the situation is not as straightforward in the case of an actuator failure. In this situation, the body may be unable to apply a force or torque in one or more of the six degrees of freedom, limiting its controllability. This is an interesting case because it is likely that an underwater vehicle loses actuator power for one reason or another and needs to return for repairs. For obvious reasons, we would like the vehicle to be able to return to home base under this distressed situation.

DEFINITION 4.2. *In this proposal, we say that a vehicle is controllable if it is able to reach any final configuration from any given initial configuration in a finite amount of time.*

Decoupling vector fields give possible trajectories which the vehicle is able to realize in the under-actuated condition. This approach to the motion planning problem stems from an example presented in *Bullo and Lynch, 2001*. There, the authors consider a single under-actuated situation in which three body-fixed control forces which are applied at a point different from C_G . They go on to show that by using only these three control forces, the vehicle is controllable. Here, we attack a slightly different problem, but the motivation is the same.

PROPOSED PROBLEM 4.3. *Given the equations of motion of a submerged rigid body as in Equations (27), we wish to compute the decoupling vector fields for each of the under-actuated scenarios including the respective external forces assumed.*

4.2 Motion Planning in an Ideal Fluid

In this section we examine the motion planning problem for the rigid body submerged in an ideal fluid through the implementation of decoupling vector fields. To find these decoupling vector fields, we examine each of the under-actuated scenarios of the rigid body.

Let $\mathcal{I}_m^{-1} = \{\tilde{\mathbb{I}}_1^{-1}, \dots, \tilde{\mathbb{I}}_m^{-1}\}$ for $m < 6$, be the set of input control vector fields to the under-actuated system. Thus, Equations (28) transform from the fully-actuated case to the the under-actuated equations of motion given by

$$\nabla_{\gamma'} \gamma'(t) = \sum_{i=1}^m \sigma_i(t) \tilde{\mathbb{I}}_i^{-1}(\gamma(t)), \quad (32)$$

with $\tilde{\mathbb{I}}_i^{-1} \in \mathbb{I}^{-1}$ and σ_i is the corresponding control.

The classification of decoupling vector fields is given with respect to the number of available degrees of freedom. First, consider the degenerate situation of a single input vector field: $m = 1$. This case can also be viewed as the loss of five degrees of freedom. Clearly the only possible motion for the body is a motion along or about one single principle axis of inertia.

DEFINITION 4.4. *The vector fields \mathbb{I}_i^{-1} for $i \in \{1, \dots, 6\}$ are called the pure motions. Their integral curves correspond to a motion along or about one single principle axis of inertia; this motion is either purely translational or purely rotational.*

In this case $\nabla_{\tilde{\mathbb{I}}_i^{-1}} \tilde{\mathbb{I}}_i^{-1} = 0$, thus the decoupling vector fields for the single input system $\nabla_{\gamma'} \gamma'(t) = \tilde{\mathbb{I}}_i^{-1}(\gamma(t)) \sigma_i(t)$ are just multiples of the input vector field $\tilde{\mathbb{I}}_i^{-1}$.

A similar analysis has been performed by the candidate to produce the decoupling vector fields for $m = 2, 3, 4, 5, 6$, however we omit this lengthy derivation and refer the interested reader to *Catone et al., 2007* for the details. For this and the following sections, we will need two definitions related to decoupling vector fields to discuss motion planning.

DEFINITION 4.5. *A vector field V is called an axial motion if it is of the form $V = h_i \mathbb{I}_i^{-1} + h_{i+3} \mathbb{I}_{i+3}^{-1}$ where $i \in \mathcal{U}$.*

We use the term axial motions since these are a translation and rotation acting on the same principle axis of inertia. These can be seen as an extension of the pure motions.

DEFINITION 4.6. *A vector field V is called a coordinate motion if it is of the form $V = h_i \mathbb{I}_i^{-1} + h_j \mathbb{I}_j^{-1} + h_k \mathbb{I}_k^{-1}$ where $i = 1$ or 4 , $j = 2$ or 5 and $k = 3$ or 6 .*

For an affine connection control system as in Equation (32), the candidate has computed decoupling vector fields for each of the under-actuated scenarios for the submerged rigid body in an ideal fluid *Chyba et al., 2007a*. We will use these results to help design trajectories and give some solutions to the motion planning problem.

In the case in which the system is fully actuated, the motion planning problem is trivial. Any two configurations can be connected simply through the use of a concatenation of pure motions. At the other extreme, when only one degree of freedom is available, the rigid body is restricted to movement along or about a single principle axis of inertia. Next, we present two examples to demonstrate the use of decoupling vector fields to give solutions to the motion planning problem in an ideal fluid when considering under-actuation.

As with the rest of this proposal, we will consider ODIN as the test-bed AUV. She is controlled by eight external thrusters; four vertical and four horizontal. Note that the majority of AUVs are controlled using external thrusters, movable wings, foils and rudders. Since actuation of movable wings, foils and rudders implies an applied force or torque to the vehicle, without loss of generality, we can assume that the vehicle is controlled strictly via external thruster actuation. Thus ODIN is an acceptable general example of a test-bed AUV.

We shall call a thruster oriented such that the output force is parallel to the (body-frame) z-axis a *vertical* thruster, and a thruster oriented such that the output force is perpendicular to the (body-frame) z-axis a

horizontal thruster. Clearly, a vertical thruster contributes to heave, roll and pitch controls, while a horizontal thruster contributes to surge, sway and yaw controls. Suppose we begin with a fully-actuated submersible which controls heave, roll and pitch with one set thrusters we will call V. While surge, sway, and yaw are controlled with another set of thrusters called H. In order to utilize the notion of decoupling vector fields in the under-actuated situation, suppose we lose the ability to control either H or V. In ODIN's situation, V represents the set of four vertical thrusters while H represents the set of four horizontal thrusters. Losing V would limit the motion of the vehicle to a plane in \mathbb{R}^3 . However, losing H would not affect the controllability of the vehicle, as we will show in the examples below. Thus, in the design process of the vehicle, we could save money by requiring that robustness or redundancy need only be implemented onto a portion of the system; the V thrusters. Also, for energy conservation, it may be better to use only one set of thrusters to save battery life. This knowledge and ability to pre-plan can save time and money for the AUV designer and end-user alike.

Now, we demonstrate two practical applications of decoupling vector fields to the motion planning problem. Suppose that we want to start at the origin ($\eta_0 = (0, 0, 0, 0, 0, 0)$) and end at $\eta_{final} = (4, 3, 2, 0, 0, -90^\circ)$. Positive b values are in the direction of gravity.

For the first example, suppose we have a vehicle designed as above. Also suppose that we are only able to control the V thrusters. In particular, we are only able to directly control heave, roll and pitch, and the input vector fields are $\mathcal{I}_3^{-1} = \{\mathbb{I}_3^{-1}, \mathbb{I}_5^{-1}, \mathbb{I}_6^{-1}\}$. By computations carried out by the candidate, we know that the decoupling vector fields for this system are the pure vector fields, $V = h_i \mathbb{I}_i^{-1}$ for $i \in \{3, 5, 6\}$. This means that the trajectory can be fully decoupled into a concatenation of pure motions. The basic idea to realize this displacement is use the pitch and roll controls to point the bottom of the vehicle in the direction of η_{final} and then use pure heave for the translational displacement. Upon reaching $(4, 3, 2, \phi, \theta, \psi)$ we can do pitch and roll movements to realize η_{final} . For this example, the vehicle needs to apply a pure pitch to reach $\tan^{-1}(\frac{3}{2})^\circ = 56.3^\circ$, pure roll to reach $-\tan^{-1}(2)^\circ = -63.4^\circ$, then translate $\sqrt{2^2 + \sqrt{4^2 + 3^2}} = 3$ units using pure heave. Now, the vehicle has position $\eta = (4, 3, 2, -63.4^\circ, 56.3^\circ, 0)$. To reach η_{final} we have two choices. First we could apply the opposite roll and pitch controls as above to set roll and pitch angles to zero, then apply a 90° pure pitch followed by a -90° pure roll followed by a -90° pure pitch. This concatenation results in a -90° yaw, and the motion is realized. Or, we could simply apply a pure pitch to reach $(4, 3, 2, -63.4^\circ, 90^\circ, 0)$, then apply a pure roll to reach $(4, 3, 2, -90^\circ, 90^\circ, 0)$ and finally a -90° pure pitch to realize η_{final} . Since we have direct control on pitch and roll for this example, it should be clear that any other rotational configuration is also possible. Thus, it is clear that the vehicle is controllable through the concatenation of decoupling vector fields. The motion of the vehicle is displayed in Figure 3. For the second example, suppose that we are only able to control the H thrusters on the vehicle. Additionally, we assume that the vehicle has a separate system to control buoyancy which is still in operation. This assumption is practically valid, and also creates a non-trivial example. In particular, we are able to directly control surge, sway, heave, and yaw; the input vector fields are $\mathcal{I}_4^{-1} = \{\mathbb{I}_1^{-1}, \mathbb{I}_2^{-1}, \mathbb{I}_3^{-1}, \mathbb{I}_6^{-1}\}$. By computations carried out by the candidate, we know that the vehicle is not controllable. Clearly, we are able to realize any position in \mathbb{R}^3 , but the vehicle is not able to achieve any angular displacements in roll or pitch. Note, the vehicle could definitely return home in a distressed situation, but it is not performing any fancy maneuvers. The decoupling vector fields for this system are the pure vector fields $V_i = h_i \mathbb{I}_i^{-1}$ for $i \in \{1, 2, 3, 6\}$, the axial vector field, $V_a = h_3 \mathbb{I}_3^{-1} + h_6 \mathbb{I}_6^{-1}$ and the coordinate vector field $V_b = h_1 \mathbb{I}_1^{-1} + h_2 \mathbb{I}_2^{-1} + h_6 \mathbb{I}_6^{-1}$. This means that the trajectory must follow the integral curves of V_a , V_b and V_i , $i \in \{1, 2, 3, 6\}$ for motion planning. The basic idea to realize this motion is to realize the angular displacement while travelling along the diagonal from $(0, 0, 0, 0, 0, 0)$ to $(4, 3, 0, 0, 0, 0)$, then apply a pure heave to reach η_{final} . For this example, the vehicle first needs to follow the integral curves of $V_b = h_1 \mathbb{I}_1^{-1} + h_2 \mathbb{I}_2^{-1} + h_6 \mathbb{I}_6^{-1}$ where $h_1 = 4$, $h_2 = 3$ and $h_6 = -\frac{\pi}{2}$. Then, we follow the integral curves of $h_3 V_3$ with $h_3 = 2$ to achieve the desired displacement. The motion of the vehicle is displayed in Figure 4.

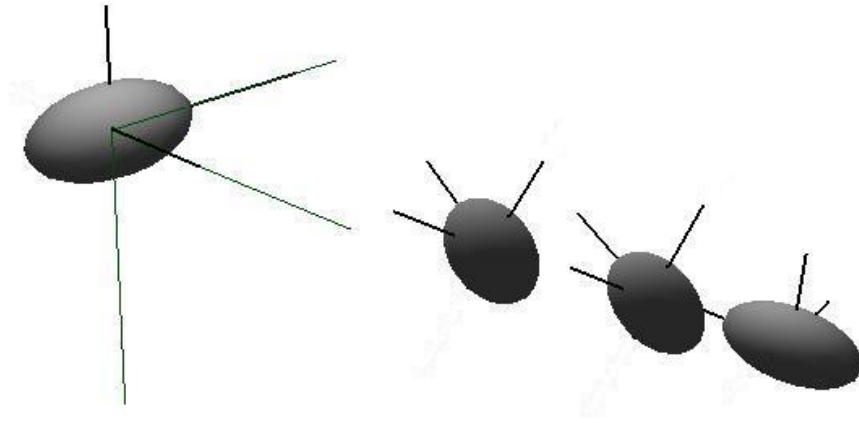


Figure 3: *Decoupling vector field trajectory using only the V thrusters, beginning at the origin and ending at $\eta_f = (4, 3, 2, 0, 0, -90^\circ)$.*

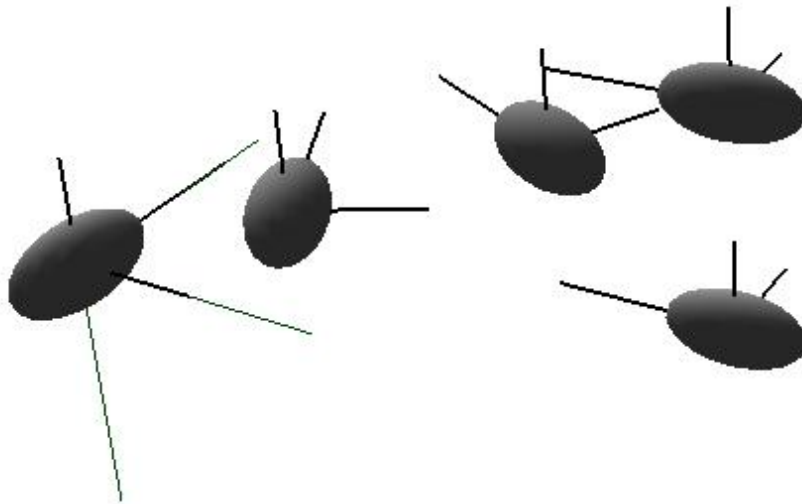


Figure 4: *Decoupling vector field trajectory using only the H thrusters, beginning at the origin and ending at $\eta_f = (4, 3, 2, 0, 0, -90^\circ)$.*

4.3 Extension to a Real Fluid

For the remainder of this proposal, we reconsider the rigid body submerged in a real fluid and consider the dissipative and potential forces acting on the system. We use Equations (23) and (26) as governing equations for the system, depending on the included forces acting upon the rigid body. It is of interest to note that the ideas discussed in the previous two sections have not been extended to the real fluid case. In particular, the notion of a kinematic reduction, and hence decoupling vector field, has not been demonstrated for forced affine connection control systems. It is a goal of this research to provide such an extension and characterization.

4.3.1 Including Drag

In Sections 2.3 and 2.4, we presented the equations of motion for the rigid body submerged in a real fluid and an ideal fluid using the Levi-Civita affine connection. We compute decoupling vector fields for a test-bed AUV submerged in an ideal fluid without external forces. For practical application concerns, we wish to apply the theory of kinematic reductions and decoupling vector fields to the forced affine connection control system. However, given the form of Equation (26), we are unable to directly apply the results of the previous sections; the external forces add a drift vector field to the geometrical acceleration. However, we may be able to express the external drag force as an intrinsic property of the affine connection as opposed to an external drift vector field of the control system. Including the drag in this way hinges upon the fact that the drag force is quadratic with respect to velocity. The candidate is actively researching this extension.

4.3.2 Including Potential Forces

Practically thinking for an AUV, it is not optimal to have $C_B = C_G$. The vehicle is quite controllable but is neutrally stable, and thus lacks any restoring moments. This means that any parasite thrusts will induce torques on the body which are not counteracted. This situation makes the body very sensitive to unbalanced thrusts; a practical problem since no two physical thrusters are identical. Since forces are assumed to act directly at C_G , if $|C_B - C_G| \neq 0$, then any pure translational force applied at C_G will induce a rotation, and a pure pitch or roll will be countered by a righting moment. However, we can still produce pure motions but we need control in more than one DOF. If we assume that $\eta_{init} = (0, 0, 0, 0, 0, 0)$, then along a pure surge the vehicle needs to compensate for the induced pitching moment to maintain the prescribed orientation. Thus we need at least control in two DOF (surge and pitch). Additionally, if we assume that $\eta_{init} = (0, 0, 0, \phi, \theta, \psi)$ where ϕ, θ and ψ are constants, then not only does the vehicle need to compensate for the induced pitching moment, but must also maintain the initial orientation by applying controls in roll and yaw as well. It is apparent then that the pure motions can be realized by applying control in at most four DOF for translation and three DOF for rotation. We remark here that for large righting arms and bounded controls the vehicle may be unable to achieve even small (5°) inclinations or maintain a given initial configuration.

Unlike the drag forces discussed in the previous section, the potential forces acting on the vehicle present no obvious way to eliminate them from being an external drift vector field in the equations of motion. Currently, other than guaranteeing that we have direct control upon pitch, roll and heave (assuming $C_B \neq C_G$ and not neutrally buoyant) there is no way to geometrically deal with these forces. In order to characterize the notion of a kinematic reduction for a mechanical system governed by Equations (23), we must find a way to deal with these forces. The candidate is actively pursuing this problem.

4.4 Experiments

During recent testing, we have successfully implemented pure motion and near time optimal trajectories onto ODIN. This directly corresponds to the implementation of theoretically influenced motions onto a rigid body submerged in a real fluid. Next we intend to characterize the axial and coordinate motions for the real fluid case and implement them onto ODIN. After this, we will be able to construct and implement concatenated decoupling vector field trajectories and experimentally examine the motion planning problem. As previously mentioned, the use of decoupling vector fields for solutions to the motion planning problem have an excellent application to under-actuated situations. These situations could occur in the event of actuator failure or as an energy saving technique for a fully-actuated submersible. We may also consider under-actuated scenarios which are also controllable for the design of new vehicles, since fewer thrusters means less power consumption as well as less cost to build the vehicle. This later consideration leads us to determine the minimal number of DOF actuation used to realize given motions for implementation. Due

to the transformation between ODIN's actual controls and the six DOF controls (similar for other specific AUVs) the minimal number of thrusters that ODIN will use to realize these motions needs to be determined separately.

Along with the aforementioned theoretical work to be implemented onto ODIN, there are many practical or experimental aspects which could be addressed. The first of these aspects is to gain a better understanding of the circulation current in the diving well. We have completed many drift experiments at multiple depths, but this only gives us a Lagrangian model for the current. We would also like to develop an Eulerian understanding as well in order to accurately represent this force in our theoretical model. From previous tests, we estimate the current to be quite steady and on the order of $1 \frac{m}{min}$. A good understanding and inclusion of this environmental factor will provide a good start to considering more complex and stronger current such as those found in the open ocean and actual AUV operating conditions. This is an external force other than those considered in Section 2.2. Inclusion of this force into the equations of motion will depend on the progress of previous proposed experiments and research.

Another candidate for investigation is the vehicle tether. ODIN runs in full autonomous mode, but is tethered to the shore based laptop in order to upload experiments without having to remove her from the water each time. However, the effect of the tether on both the buoyancy and motion of ODIN is not negligible. A full understanding and modelization of the tether effects is beyond the scope of this proposal, but a first approximation would increase the accuracy of experimental tests. We are currently working with ASL to construct a wireless buoy system for ODIN. A similar system is implemented on ODIN's big brother SAUVIM, and is working well to our knowledge. Even with this system in place, ODIN will not be tethered to shore, but will be connected to the floating buoy. Research into the wireless buoy system as well as the drag effects of the tether are currently under investigation.

With AUV research, an ongoing issue is always the positioning of the vehicle. As mentioned earlier, many systems have been tried but no solution has proved both accurate and cost effective for the horizontal positioning problem. Currently we are satisfied with our post-processed results from the video camera atop the 10m platform. However, it would be of great benefit to have real time feedback of horizontal position as we further the merging of theory and research. On the other hand, the orientation sensor (inertial measurement unit) is an area where we may be able to improve. The Watson sensor currently installed is very accurate, but can not keep its precision for rapid orientation changes ($> 5^\circ/sec$) and under these conditions has considerable drift ($> 10^\circ$). This causes a real tracking problem for the yaw component even when running closed loop on this control. A sensor fusion of the Watson with a Fiber Optic Gyroscope (FOG) is currently being examined for SAUVIM. We hope that some information from this research can be applied to ODIN. Again, we will work with ASL on this aspect.

4.5 Open Questions

The main question is to characterize the notion of a kinematic reduction in a real fluid, and thus determine decoupling vector fields for the forced affine-connection control system and supply necessary and sufficient conditions for a vector field to be decoupling. To this end, we will examine the under-actuated scenarios for the rigid body submerged in a real fluid subjected to dissipative and potential forces. This characterization will lead to the formalization of a kinematic reduction of rank one for the system. We also propose to investigate additional under-actuated situations for the rigid body such as forces not acting at the center of gravity. This is intended to be an extension of the example given in *Bullo and Lynch, 2001* to the real fluid case. This research should help develop a proper and complete generalization of the notion of decoupling vector fields for the forced affine-connection control system.

With this new characterization of the geometric reduction procedure, the candidate proposes to construct solutions to the motion planning problem through the concatenation of decoupling vector fields and subsequently implement these trajectories onto ODIN. These trajectories will be implemented in both the

fully and under-actuated situations. This generalization may also allow us to geometrically reformulate the numerical STPP algorithm previously developed. This reformulation will utilize the integral curves of the decoupling vector fields from the real fluid case. In this proposal we will also investigate the relationship between the singular extremals associated with an optimal control problem and the notion of decoupling vector fields for the system. This relationship is an open question in either an ideal or real fluid. Research has already been started in this area.

References

Allmendinger, E. *Submersible Vehicle Design*. SNAME, 1990.

Bertram, V. and Alvarez, A. *Hydrodynamic Aspects of AUV Design*. 5th International Conference on Computer Applications and Information Technology in the Maritime Industries, 2006.

Bhattacharyya, R. *Dynamics of Marine Vehicles*. Wiley, 1978.

Bullo, F. and Lynch, K. *Kinematic Controllability for Decoupled Trajectory Planning in Underactuated Mechanical Systems*. IEEE Transactions. Robotics and Automation, 17(4):402-412, 2001.

Bullo, F. and Lewis A. and Lynch K. *Controllable Kinematic Reductions for Mechanical Systems: Concepts, Computational Tools, and Examples*. Proceedings of MTNS02, University of Notre Dame, 2002.

Bullo, F. and Lewis, A. *Geometric Control of Mechanical Systems*. Springer, 2005.

Catone, C. and Chyba, M. and Smith, R. and Wilkens, G. *A Geometrical Approach to the Motion Planning Problem for a Submerged Rigid Body*. Preprint to be submitted to the International Journal of Control, 2007.

Chyba, M. and Haberkorn, T. and Smith, R. and Choi, S. *Implementable Efficient Time and Energy Consumption Trajectories Design for an Autonomous Underwater Vehicle*. 6th Ship Technology Research, to appear 2007, (2007a).

Chyba, M. and Haberkorn, T. and Smith, R. *Design and Implementation of Time Efficient Trajectories for Autonomous Underwater Vehicles*. Ocean Engineering, to appear 2007, (2007b).

Chyba, M. and Haberkorn, T. and Smith, R. and Wilkens, G. *Design of Time Efficient Trajectories for a Submerged Rigid Body*. Discrete and Continuous Dynamical Systems, to appear 2007, (2007c).

Do Carmo, M. *Riemannian Geometry* Birkhauser Boston, 1992.

Fossen, T. *Guidance and Control of Ocean Vehicles*. John Wiley & Sons, 1994.

Imlay, F. *The Complete Expressions for Added Mass of a Rigid Body Moving in an Ideal Fluid*. Technical Report DTMB 1528, David Taylor Model Basin, Washington D.C., 1961.

Lamb, H. *Hydrodynamics*. Dover Publications, 6th Edition, 1945.

Leonard, N. *Stability of a bottom-heavy underwater vehicle*. Automatica, 33(3):331-346, 1997.

Leonard, N. *Stabilization of Steady Motions of an Underwater Vehicle*. Proceedings of the 35th IEEE Conference on Decision and Control, 1996.

MacIver, M. and Fontaine, E. and Burdick, J. *Designing Future Underwater Vehicles: Principles and Mechanisms of the Weakly Electric Fish*. IEEE Journal of Oceanic Engineering, 29(3), July 2004.

NOAA Ocean Exploration Panel Web Site (2004), http://oceanpanel.nos.noaa.gov/panelreport/ocean_panel_report.html.